

Learning A Task-Specific Deep Architecture For Clustering

Zhangyang Wang* Shiyu Chang* Jiayu Zhou† Thomas S. Huang*

Abstract

While deep networks show to be highly effective in extensive applications, few efforts have been spent on studying its potential in clustering. In this paper, we argue that the successful domain expertise represented by the sparse code-based clustering frameworks is still valuable, and can be combined with the key ingredients of deep learning. A novel feed-forward architecture, named TAGnet, is constructed from graph-regularized sparse coding. It is then trained with task-specific loss functions from end to end. The inner connections of the proposed network to sparse coding lead to more effective training. Moreover, by introducing auxiliary clustering tasks to the hierarchy of intermediate features, we present DTAGnet and obtain a further performance boost. We demonstrate extensive experiments on several benchmark datasets, under a wide variety of settings. The results verify that the proposed model significantly outperforms the generic architectures of the same parameter complexity, and also gains remarkable margins over several state-of-the-art methods.

1 Introduction

Clustering aims to learn the hidden data patterns in an unsupervised way, and group similar patterns among massive data. Generative clustering algorithms model categories in terms of their geometric properties in feature spaces, or as statistical processes of data. Examples include K-means and Gaussian mixture model (GMM) clustering [3], which assume a parametric form of the underlying category distributions. On the other hand, discriminative clustering algorithms search for the boundaries or distinctions between categories. With fewer assumptions being made, these methods are powerful and flexible in practice. Examples include maximum-margin clustering [27], information theoretic clustering [15], and many more.

Most existing clustering algorithms work well when the data dimensionality is low. While partitioning high-dimensional data, their performances are not guaranteed. As suggested by [18], high-dimensional data exhibits dense grouping in low-dimensional embeddings. That motivates researchers to first project the original data into a low-dimensional subspace using methods such as PCA and LDA

[20], and then cluster the embedding features. Further, sparse codes [26] are proven to be robust and efficient features for clustering. Many successful sparse code-based clustering frameworks, such as [5, 30], remind us of the significance of the **domain expertise** represented by their pipelines. More recently, deep learning have attracted great attention in many feature learning and classification problems [12]. The advantages of deep learning lie in its composition of multiple non-linear transformations to yield more abstract and descriptive embedding representations. However, there has not been much attention paid to the potential of deep learning for unsupervised clustering problems. Moreover, generic deep architectures [12] learn all their knowledge from training data, while the problem-specific priors and expertise are largely ignored in learning.

Inspired by the successful practice of sparse codes in clustering [5, 30, 25], we combine the domain expertise of conventional sparse coding, with the key ingredients of deep learning, and outline a carefully crafted deep framework for clustering. Its feature extraction layers closely mimic the process of sparse coding, using a time-unfolded structure inspired from iterative algorithms [9]. The developed feed-forward neural network, named **TAGnet**, is specifically crafted to extract the sparse code-type features under graph constraints, that are also optimized under task-specific loss functions from end to end. Benefiting from both the sparse coding domain expertise and the large learning capacity of deep networks, the proposed model achieves notable improvements over the generic deep models of the same parameter complexity. Moreover, the learned intermediate representations continue to have clustering interpretations across different latent attributes [23]. By enforcing auxiliary clustering tasks on the hierarchy of features, we develop **DTAGnet** and observe further performance boosts on the CMU MultiPIE dataset [10].

2 Related Work

2.1 Sparse coding for clustering

Assuming that data samples $\mathbf{X} = [\mathbf{x}_1, \mathbf{x}_2, \dots, \mathbf{x}_n]$, $\mathbf{x}_i \in R^{m \times 1}$, $i = 1, 2, \dots, n$, are encoded into their corresponding sparse codes $\mathbf{A} = [\mathbf{a}_1, \mathbf{a}_2, \dots, \mathbf{a}_n]$, $\mathbf{a}_i \in R^{p \times 1}$, $i = 1, 2, \dots, n$, using a learned dictionary $\mathbf{D} = [\mathbf{d}_1, \mathbf{d}_2, \dots, \mathbf{d}_p]$, where $\mathbf{d}_i \in R^{m \times 1}$, $i = 1, 2, \dots, p$ are the learned atoms. The sparse codes are obtained by solving the following convex

*Beckman Institute, University of Illinois at Urbana-Champaign, IL 61821. {zwang119, chang87, t-huang1}@illinois.edu.

†Department of Computer Science and Engineering, Michigan State University, MI 48824. jiyuz@msu.edu

optimization (λ is a constant):

$$(2.1) \quad \mathbf{A} = \arg \min_{\mathbf{A}} \frac{1}{2} \|\mathbf{X} - \mathbf{D}\mathbf{A}\|_F^2 + \lambda \sum_i \|\mathbf{a}_i\|_1$$

In [5], the authors suggested that the sparse codes can be used to constitute the similarity graph for spectral clustering [17]. Furthermore, to capture the geometric structure of local data manifolds, the graph regularized sparse codes are further suggested in [30, 28], by solving:

$$(2.2) \quad \mathbf{A} = \arg \min_{\mathbf{A}} \frac{1}{2} \|\mathbf{X} - \mathbf{D}\mathbf{A}\|_F^2 + \lambda \sum_i \|\mathbf{a}_i\|_1 + \frac{\alpha}{2} \text{Tr}(\mathbf{A}\mathbf{L}\mathbf{A}^T),$$

where \mathbf{L} is the graph Laplacian matrix and can be constructed from a pre-chosen pairwise similarity matrix \mathbf{P} . More recently in [25], the authors suggested to simultaneously learn feature extraction and discriminative clustering, by formulating a task-driven sparse coding model [16]. They proved that the joint methods consistently outperformed non-joint counterparts.

2.2 Deep learning for clustering In [22], the authors first explored the possibility of employing deep learning in graph clustering. They first learned a nonlinear embedding of the original graph by the auto encoder (AE), and then runs K-means algorithm on the embedding to obtain clustering result. Being very straightforward, it neither exploits more adapted deep architectures nor performs any task-specific joint optimization. In [4], a deep belief network (DBN) [11] with nonparametric clustering was presented. As a generative graphical model, DBN allows for fast feature learning but is usually not as effective as AEs in learning discriminative features for clustering. In [23], the authors extended the semi non-negative matrix factorization (Semi-NMF) model [14] to a Deep Semi-NMF model, whose architecture resembles AEs.

3 Model Formulation

The proposed pipeline consists of two blocks, and is trained end-to-end in an unsupervised way, as depicted in Fig. 1 (a). A feed-forward architecture, Task-specific And Graph-regularized Network (TAGnet), is adopted to extract discriminative features, on top of which clustering-oriented loss functions are enforced.

3.1 TAGnet: Task-specific And Graph-regularized Network The close connection has been noticed between sparse coding and neural network. In [9], a feed-forward neural network is proposed to efficiently approximate the sparse code \mathbf{a} of input signal \mathbf{x} , which is obtained by solving (2.1) in advance. The network, named learned ISTA (LISTA), is a network implementation of the iterative shrinkage and thresholding algorithm (ISTA). The authors of [9] learned the network parameters as a general regression model from

training data to their pre-solved sparse codes, using a back-propagation algorithm.

While LISTA is proven to be an efficient and flexible implementation of conventional sparse coding (2.1), it assumes the “optimal” sparse codes to be pre-obtained from (2.1), which implicitly requires that the dictionary \mathbf{D} is estimated [9]. In that way, LISTA could only serve as a sparse code predictor for input vectors drawn from the same distribution as the training samples, whose effectiveness further hinges on the choice of \mathbf{D} . Moreover, LISTA overlooks the useful geometric information among data points [30].

We hereby propose Task-specific And Graph-regularized Network (TAGnet) to learn effective features for clustering, which is superior in two folds:

- TAGnet learns feature optimized under clustering criteria. While LISTA merely minimizes the approximation error to the optimal sparse codes on a given dataset, TAGnet produces more discriminative features as well as avoids the tedious pre-computation of \mathbf{A} .
- TAGnet encodes the graph constraint in (2.2) to further regularize the solution. Previous results [30] indicate that encoding geometrical information will significantly enhance the clustering performances.

TAGnet is derived from the following theorem:

THEOREM 3.1. *The optimal sparse code \mathbf{A} from (2.2) is the fixed point of*

$$(3.3) \quad \mathbf{A} = h_{\frac{\lambda}{N}} \left[\left(\mathbf{I} - \frac{1}{N} \mathbf{D}^T \mathbf{D} \right) \cdot \mathbf{A} - \mathbf{A} \cdot \left(\frac{\alpha}{N} \mathbf{L} \right) + \frac{1}{N} \mathbf{D}^T \mathbf{X} \right],$$

where h_{θ} is an element-wise shrinkage function:

$$(3.4) \quad [h_{\theta}(\mathbf{u})]_i = \text{sign}(\mathbf{u}_i) (|\mathbf{u}_i| - \theta)_+$$

N is an upper bound on the largest eigenvalue of $\mathbf{D}^T \mathbf{D}$.

The complete proof of Theorem 3.1 can be found in the supplementary. Theorem 3.1 outlines an iterative algorithm to solve (2.2). Under quite mild conditions [2], after \mathbf{A} is initialized, one may repeat the shrinkage and thresholding process in (3.3) until convergence. The iterative algorithm could be alternatively expressed as the block diagram in Fig. 1 (b), where

$$(3.5) \quad \mathbf{W} = \frac{1}{N} \mathbf{D}^T, \mathbf{S} = \mathbf{I} - \frac{1}{N} \mathbf{D}^T \mathbf{D}, \theta = \frac{\lambda}{N}.$$

In particular, we define the new operator “ $\times \mathbf{L}$ ”: $\mathbf{A} \rightarrow -\frac{\alpha}{N} \mathbf{A} \mathbf{L}$.

By time-unfolding and truncating Fig. 1 (b) to a fixed number of K iterations ($K = 2$ by default)¹, we obtain the

¹We test larger K values (3 or 4), but they do not bring noticeable performance improvements in our clustering cases.

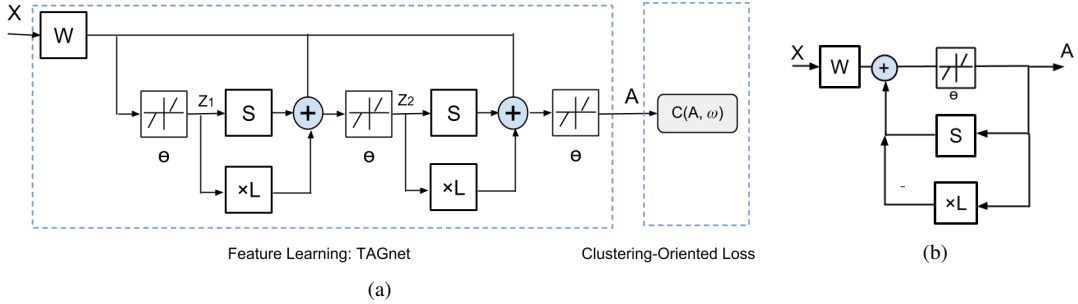


Figure 1: (a) The proposed pipeline, consisting of the TAGnet network for feature learning and the clustering-oriented loss functions on its top. The parameters \mathbf{W} , \mathbf{S} , θ and ω are all learnt from training data from end to end. (b) The block diagram of solving (3.3).

TAGnet form of the first block in Fig. 1 (a). \mathbf{W} , \mathbf{S} and θ are all to be learnt jointly from data. We are motivated from the fixed point iteration algorithm as in Fig. 1 (b), and share \mathbf{W} , \mathbf{S} and θ for both stages². Compared to the linear layers \mathbf{W} and \mathbf{S} , the activation thresholds θ are less straightforward to be updated. To facilitate training, we rewrite (3.4) as:

$$[h_{\theta}(\mathbf{u})]_i = \theta_i \cdot \text{sign}(\mathbf{u}_i) (|\mathbf{u}_i|/\theta_i - 1)_+ = \theta_i h_1(\mathbf{u}_i/\theta_i)$$

Eqn. (3.6) indicates that the original neuron with trainable thresholds can be decomposed into two linear scaling layers plus a unit-threshold neuron. The weights of the two scaling layers are diagonal matrices defined by θ and its element-wise reciprocal, respectively.

The graph laplacian \mathbf{L} in the new $\times \mathbf{L}$ term could be readily obtained in advance. In each stage, the $\times \mathbf{L}$ branch will execute feed-forward computation by taking the intermediate \mathbf{Z}_k ($k = 1, 2$) as its input. Its output is to be aggregated from the output of the learnable \mathbf{S} layer. However, \mathbf{L} itself will not be altered by back propagations.

An appealing highlight of (D)TAGnet lies in its very effective and straightforward **initialization strategy**. While many neural networks train well with random initializations without pre-training, given the training data is sufficient, it has been discovered that poorly initialized networks has hampered the effectiveness of first-order methods (e.g., SGD) in certain cases [21]. For (D)TAGnet, it is however much easier to initialize the model in the right regime, benefiting from the **analytical relationships between sparse coding and network hyperparameters** defined in (3.5). That is especially meaningful when clustering on relatively small-scale datasets, e.g., COIL 20.

In sum, the graph-regularized sparse coding prior is effectively encoded in the TAGnet structure, while all parameters can be learned jointly through back-propagation. Rather

than to predict the solution of (2.2) exactly as in LISTA [9], the goal of TAGnet is instead to learn discriminative embedding that is optimal for clustering. Therefore, the output \mathbf{A} of TAGnet is not necessarily identical (or even close) to the predicted sparse codes by solving (2.2). By slightly abusing the notation \mathbf{A} in (2.2) here, we intend to remind the close analytical relationship (but not equivalence) between TAGnet and (2.2), that makes the whole model more interpretable. It also provides us with a clue on model initialization.

3.2 Clustering-oriented loss functions Assuming K clusters, and $\omega = [\omega_1, \dots, \omega_K]$ as the set of parameters of the loss function, where ω_i corresponds to the i -th cluster, $i = 1, 2, \dots, K$. A natural choice of the loss function is extended from the popular softmax loss in supervised learning [12], and take the entropy-like form:

$$(3.7) \quad C(\mathbf{A}, \omega) = - \sum_{i=1}^n \sum_{j=1}^K p_{ij} \log p_{ij}.$$

where p_{ij} denotes the the confidence probability that sample \mathbf{x}_i belongs to cluster j , $i = 1, 2, \dots, N$, $j = 1, 2, \dots, K$:

$$(3.8) \quad p_{ij} = p(j|\omega, \mathbf{a}_i) = \frac{e^{-\omega_j^T \mathbf{a}_i}}{\sum_{t=1}^K e^{-\omega_t^T \mathbf{a}_i}},$$

In testing, the predicted cluster label of \mathbf{a}_i is the cluster j where it achieves the largest likelihood probability p_{ij} .

In [27], the authors proposed maximum margin clustering (MMC), which borrows the idea from the theory of SVM [6]. MMC finds a way to label the samples by running an SVM implicitly, and the SVM margin obtained would be maximized over all possible labels [29]. By referring to the MMC definition, the authors of [25] designed the max-margin loss:

$$(3.9) \quad C(\mathbf{A}, \omega) = \frac{\lambda}{2} \|\omega\|^2 + \sum_{i=1}^n C(\mathbf{a}_i, \omega).$$

In the above equation, the loss for an individual sample \mathbf{a}_i is

²Out of curiosity, we have also tried the architecture that treat \mathbf{W} , \mathbf{S} and θ in both stages as independent variables. We find that sharing parameters improves the performance.

defined as:

$$(3.10) \quad \begin{aligned} C(\mathbf{a}_i, \boldsymbol{\omega}) &= \max(0, 1 + f^{r_i}(\mathbf{a}_i) - f^{y_i}(\mathbf{a}_i)) \\ \text{where } y_i &= \arg \max_{j=1, \dots, K} f^j(\mathbf{a}_i) \\ r_i &= \arg \max_{j=1, \dots, K, j \neq y_i} f^j(\mathbf{a}_i). \end{aligned}$$

where f^j is the prototype for the j -th cluster. The predicted cluster label of \mathbf{a}_i is the cluster of the weight vector that achieves the maximum value $\boldsymbol{\omega}_j^T \mathbf{a}_i$.

Model Complexity The proposed framework can handle large-scale and high-dimensional data effectively via the stochastic gradient descent (SGD) algorithm. In each step, the back propagation procedure requires only operations of order $O(p)$ [9]. The training algorithm takes $O(Cnp)$ time (C is the constant absorbing epochs, stage numbers, etc.). In addition, whereas graph regularized sparse coding (2.2) is hard to be parallel, SGD is easy to be parallelized.

4 A Deeper Look: Hierarchical Clustering by DTAGnet

Deep networks are renowned for their capabilities to learn semantically rich representations by hidden layers, that call for task-specific interpretations [7]. In this section, we investigate how the intermediate features \mathbf{Z}_k ($k = 1, 2$) in TAGnet (Fig. 1 (a)) can be interpreted, and further utilized to improve the model, for specific clustering tasks. Compared to related non-deep models [25], such a hierarchical clustering property is another unique advantage of being deep.

Our strategy is mainly inspired by the algorithmic framework of deeply supervised nets [13]. As in Fig. 2, our proposed Deeply-Task-specific And Graph-regularized Network (**DTAGnet**) brings in additional deep feedbacks, by associating a clustering-oriented local auxiliary loss $C_k(\mathbf{Z}_k, \boldsymbol{\omega}_k)$ ($k = 1, 2$) with each stage. Such an auxiliary loss takes the same form as the overall $C(\mathbf{A}, \boldsymbol{\omega})$, except that the expected cluster number may be different, depending on the auxiliary clustering task to be performed. The DTAGnet backpropagates errors not only from the overall loss layer, but also simultaneously from the auxiliary losses.

While seeking the optimal performance of the target clustering, DTAGnet is also driven by two auxiliary tasks that are explicitly targeted at clustering specific attributes. It enforces constraint at each hidden representation for directly making a good cluster prediction. In addition to the overall loss, the introduction of auxiliary losses gives another strong push to obtain discriminative and sensible features at each individual stage. As discovered in the classification experiments in [13], the auxiliary loss both acts as feature regularization to reduce generalization errors and results in faster convergence. We also find in Section V that every \mathbf{Z}_k ($k = 1, 2$) is indeed most suited for its targeted task.

In [23], a Deep Semi-NMF model was proposed to learn hidden representations, that grant themselves an interpretation of clustering according to different attributes. The au-

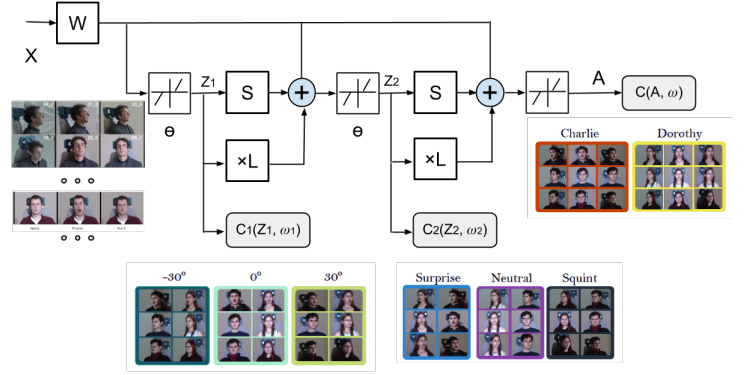


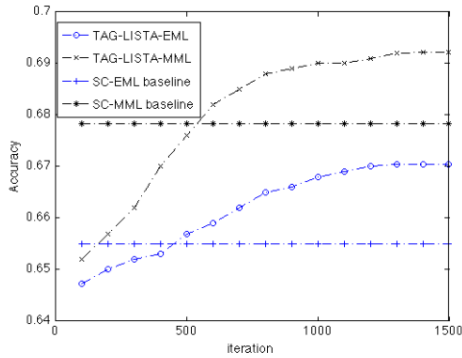
Figure 2: The DTAGnet architecture, taking the CMU MultiPIE dataset as an example. The model is able to simultaneously learn features for pose clustering (\mathbf{Z}_1), for expression clustering (\mathbf{Z}_2), and for identity clustering (\mathbf{A}). The first two attributes are related to and helpful for the last (overall) task. Part of image sources are referred from [10] and [23].

thors considered the problem of mapping facial images to their identities. A face image also contains attributes like pose and expression that help identify the person depicted. In their experiments, the authors found that by further factorizing this mapping in a way that each factor adds an extra layer of abstraction, the deep model could automatically learn latent intermediate representations that are implied for clustering identity-related attributes. Although there is a clustering interpretation, those hidden representations are not specifically optimized in clustering sense. Instead, the entire model is trained with only the overall reconstruction loss. Consequently, their clustering performance is not satisfactory. Our study shares the similar observation and motivation with [23], but in a more task-specific manner by performing the optimizations of auxiliary clustering tasks jointly with the overall task.

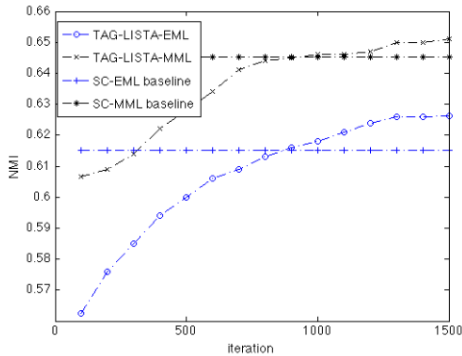
5 Experiment Results

5.1 Datasets and measurements We evaluate the proposed model on clustering three datasets, including:

- **MNIST** consists of a total number of 70, 000 quasi-binary, handwritten digit images, with digits 0 to 9. The digits are normalized and centered in fixed-size images of 28×28 .
- **CMU MultiPIE** contains around 750, 000 images of 337 subjects, captured under varied laboratory conditions. A unique property of CMU MultiPIE lies in that each image comes with labels for the identity, illumination, pose and expression attributes. That is why CMU MultiPIE is chosen in [23] to learn multi-attribute fea-



(a) Accuracy versus iteration number



(b) NMI versus iteration number

Figure 3: The accuracy and NMI plots of TAGnet-EML/TAGnet-MML on MNIST, starting from the initialization, and tested every 100 iterations. The accuracy and NMI of SC-EML/SC-MML are also plotted as baseline references.

tures (Fig. 2) for hierarchical clustering. In our experiments, we follow [23] and adopt a subset of 13, 230 images of 147 subjects in 5 different poses and 6 different emotions. Notably, we do not pre-process the images by using piece-wise affine warping as utilized by [23] to align these images.

- **COIL20** contains 1, 440 32×32 gray scale images of 20 objects (72 images per object). The images of each object were taken 5 degree apart as the object is rotated on a turntable.

Although the paper only evaluates the proposed method using image datasets, the methodology itself is not limited to only image subjects. We apply two widely-used measures to evaluate the clustering performances: the accuracy and the Normalized Mutual Information(NMI) [30], [5].

5.2 Experiment settings The proposed networks are implemented using the cuda-convnet package [12]. The network takes $K = 2$ stages by default. We apply a constant

learning rate of 0.01 with no momentum to all trainable layers, as well as a batch size of 128. In particular, to encode graph regularization as a prior, we fix \mathbf{L} during model training by setting its learning rate to be 0. The clipping is performed [19] on the gradients with a threshold of 1. For the graph regularization. Experiments run on a workstation with 12 Intel Xeon 2.67GHz CPUs and 1 GTX680 GPU. The training takes approximately 1 hour on the MNIST dataset. It is also observed that the training efficiency of our model scales approximately linearly with data.

In our experiments, we set the default value of α to be 5, p to be 128³, and λ to be chosen from [0.1, 1] by cross-validation. A dictionary \mathbf{D} is first learned from \mathbf{X} by K-SVD [1]. \mathbf{W} , \mathbf{S} and θ are then initialized based on (3.5). \mathbf{L} is also pre-calculated from \mathbf{P} , which is formulated by the Gaussian Kernel: $\mathbf{P}_{ij} = \exp(-\frac{\|\mathbf{x}_i - \mathbf{x}_j\|_2^2}{\delta^2})$ (δ is also selected by cross-validation). After obtaining the output \mathbf{A} from the initial (D)TAGnet models, ω (or ω_k) could be initialized based on minimizing (3.7) or (3.9) over \mathbf{A} (or \mathbf{Z}_k).

5.3 Comparison experiments and analysis

5.3.1 Benefits of the task-specific deep architecture

We denote the proposed model of TAGnet plus entropy-minimization loss (EML) (3.7) as TAGnet-EML, and the one plus maximum-margin loss (MML) (3.9) as TAGnet-MML, respectively. We refer to the initializations of the proposed joint models as their “non-joint” counterparts, denoted as NJ-TAGnet-EML and NJ-TAGnet-MML (NJ short for non-joint), respectively.

To verify the important argument that *the proposed model benefits from the task-specific TAGnet architecture, rather than just the large learning capacity of generic deep models*, we design a **Baseline Encoder** (BE) for comparison, which is a fully-connected feedforward network, consisting of three hidden layers of dimension p with ReLU neurons. It is obvious that the baseline encoder thus has the *same parameter complexity* as TAGnet⁴. The BEs are also tuned by EML or MML in the same way, denoted as BE-EML or BE-MML, respectively.

Moreover, we compare the proposed models with their closest “shallow” competitors, i.e., the joint optimization methods of graph-regularized sparse coding and discriminative clustering described in [25]. We re-implement their work using both (3.7) or (3.9) losses, denoted as SC-EML and SC-MML (SC short for sparse coding). Since in [25] the authors already revealed SC-MML outperforms the classical methods such as MMC and ℓ_1 graph methods, we do not

³The default values of α and p are inferred from the related sparse coding literature[30], and validated in experiments.

⁴except for the “ θ ” layers, each of which contains only p free parameters and thus ignored

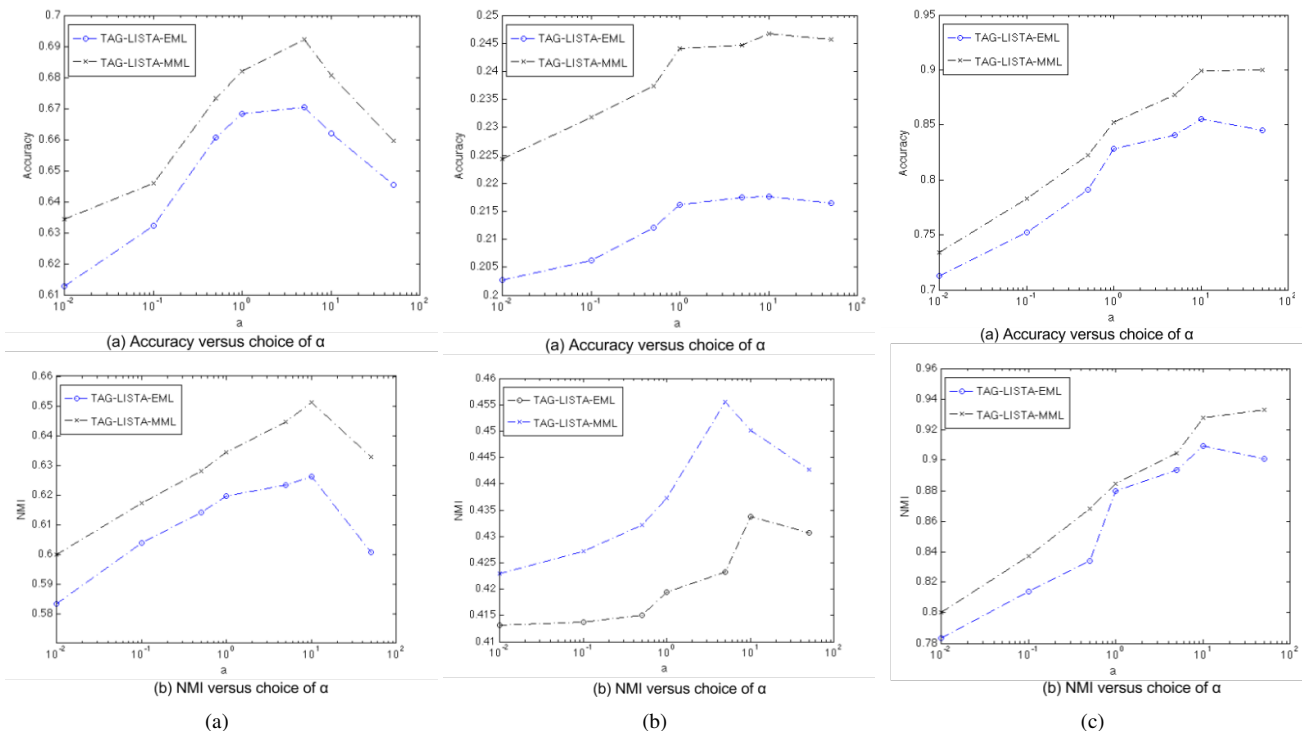


Figure 4: The clustering accuracy and NMI plots (x-axis logarithm scale) of TAGnet-EML/TAGnet-MML versus the parameter choices of α , on: a) MNIST; b) CMU MultiPIE; c) COIL20.

compare with them again. In addition, we also include Deep Semi-NMF [23] as one state-of-the-art deep learning-based clustering work.⁵

As revealed by the full comparison results in Table 1, the proposed task-specific deep architectures outperform other with noticeable margins, partially owing to the underlying domain expertise that guides the data-driven training in a more principled way. In contrast, the “general-architecture” baseline encoders (BE-EML and BE-MML), which have the same parameter complexity, appear to produce much worse (even worst) results. On the other hand, it is evident that the proposed end-to-end optimized models each outperform their “non-joint” fellows. For example, on the MNIST dataset, TAGnet-MML surpasses NJ-TAGnet-MML by around 4% in accuracy and 5% in NMI.

When comparing the TAGnet-EML/TAGnet-MML with SC-EML/SC-MML, we draw the convincing conclusion, that adopting a more parameterized deep architecture allows for a larger feature learning capacity compared to conventional sparse coding. Although similar points are well made in many other fields [12], we are interested in a closer look between the two. Fig. 3 plots the clustering accuracy and

NMI curves of TAGnet-EML/TAGnet-MML on the MNIST dataset, along with iteration numbers. Each model is well initialized at the very beginning, and the clustering accuracy and NMI are computed every 100 iterations. At first, the clustering performances of deep models are even slightly worse than sparse-coding methods, mainly since the initialization of TAGnet hinges on a truncated approximated of graph-regularized sparse coding. After a small number of iterations, the performance of each model surpasses sparse coding very soon, and continue rising monotonically until reaching a higher plateau.

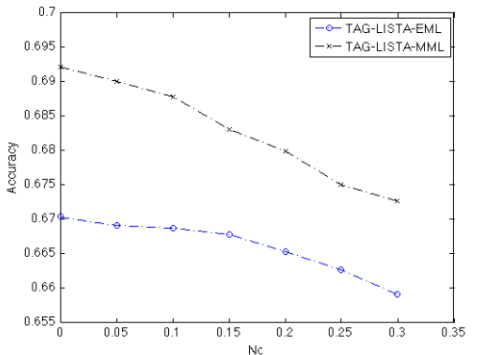
5.3.2 Effects of graph regularization In (2.2), the graph regularization term imposes stronger smoothness constraints on the sparse codes with larger α , and the same way in TAGnet. We investigate how the clustering performances of TAGnet-EML/TAGnet-MML are influenced by various α values. From Fig. 4, we observe the identical general tendency on all three datasets, that while α increases, the accuracy/NMI result will first rise then decrease, with the peak appearing between $\alpha \in [5, 10]$ (thus we choose $\alpha = 5$ as the default value). As an interpretation, the local manifold information is not sufficiently encoded when α is too small ($\alpha = 0$ will completely disable the $\times \mathbf{L}$ branch of TAGnet). On the other hand, when α turns overly large, the sparse

⁵We compare our results with their reported performance numbers on CMU MultiPIE. With various component numbers tested in [23], we choose the best results (60 components).

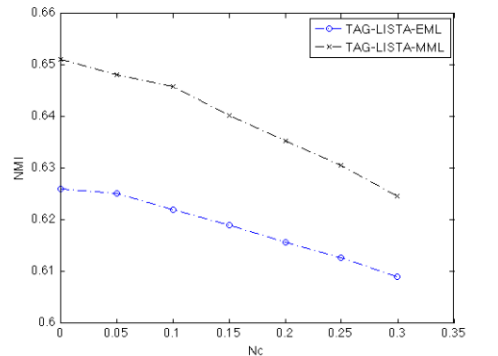
Table 1: Accuracy and NMI performance comparisons on all three datasets

		TAGnet -EML	TAGnet -MML	NJ-TAGnet -EML	NJ-TAGnet -MML	BE -EML	BE -MML	SC -EML	SC -MML	Deep Semi-NMF
<i>MNIST</i>	Acc	0.6704	0.6922	0.6472	0.5052	0.5401	0.6521	0.6550	0.6784	/
	NMI	0.6261	0.6511	0.5624	0.6067	0.5002	0.5011	0.6150	0.6451	/
<i>CMU MultiPIE</i>	Acc	0.2176	0.2347	0.1727	0.1861	0.1204	0.1451	0.2002	0.2090	0.17
	NMI	0.4338	0.4355	0.3167	0.3284	0.2672	0.2821	0.3337	0.3521	0.36
<i>COIL20</i>	Acc	0.8553	0.8991	0.7432	0.7882	0.7441	0.7645	0.8225	0.8658	/
	NMI	0.9090	0.9277	0.8707	0.8814	0.8028	0.8321	0.8850	0.9127	/

codes are “over-smoothened” with a reduced discriminative ability. Note similar phenomena are also reported in other relevant literature, e. g. , [30, 25].



(a) Accuracy versus N_c



(b) NMI versus N_c

Figure 5: The clustering accuracy and NMI plots of TAGnet-EML/TAGnet-EML versus the cluster number N_c ranging from 2 to 10, on MNIST.

On the other hand, comparing among Fig. 4 (a), (b) and (c), it is noteworthy to observe how graph regularization behaves differently on three of them. We notice that the COIL20 dataset is most sensitive to the choice of α , and increasing α from 0.01 to 50 leads to an improvement of more than 10%, in terms of both accuracy and NMI, for both TAGnet-EML and TAGnet-MML. It verifies the significance of graph regularization when applied to small-scale, high-dimensional datasets [28]. On the MNIST dataset, both

models obtain a gain of up to 6% in accuracy and 5% in NMI, by tuning α from 0.01 to 10. However, unlike COIL20 that almost always favors larger α , the model performance on the MNIST dataset tends to be not only saturated, but even significantly hampered when α continues rising to 50. The CMU MultiPIE dataset witnesses moderate improvements of around 2% in both measurements. It seems not as sensitive to α in our experiments, potentially due to the complex variability in original images that makes the graph \mathbf{W} unreliable for estimating the underlying manifold geometry. We suspect that more sophisticated graphs may help alleviate the problem, and will explore it in future.

5.3.3 Scalability and robustness On the MNIST dataset, We re-conduct the clustering experiments with the cluster number N_c ranging from 2 to 10, using TAGnet-EML/TAGnet-MML. For each N_c except for 10, 10 test runs are conducted on different randomly chosen clusters, and the final scores are obtained by averaging over the tests. Fig. 5 shows the clustering accuracy and NMI measurements versus the number of clusters. The clustering performance transits smoothly and robustly when the task scale changes.

To examine the proposed models’ robustness to noise, we add various Gaussian noise, whose standard deviation s ranges from 0 (noiseless) to 0.3, to the MNIST data, and then re-train our model. Fig. 6 indicates that both TAGnet-EML and TAGnet-MML own certain robustness to noise. When s is less than 0.1, there is even little visible performance degradation. While TAGnet-MML constantly outperforms TAGnet-EML in all our experiments (as MMC is well-known to be highly discriminative [27]), it is interesting to observe in Fig. 6 that the latter is slightly more robust to noise than the former, perhaps because the probability-driven loss form (3.7) of EML allows for more flexibility.

5.4 Hierarchical clustering on CMU MultiPIE As observed, CMU MultiPIE remains very challenging for the basic identity clustering task. However, it comes with several other attributes: pose, expression, and illumination, which could be of assistance in our proposed DTAGnet framework. In this section, we adopt the similar setting suggested in [23] applied on the same CMU MultiPIE subset, setting pose clustering as the Stage I auxiliary task, and expression clus-

tering as the Stage II auxiliary task⁶. In that way, we target $C_1(\mathbf{Z}_1, \omega_1)$ at 5 clusters, $C_2(\mathbf{Z}_2, \omega_2)$ at 6 clusters, and finally $C(\mathbf{A}, \omega)$ as 147 clusters.

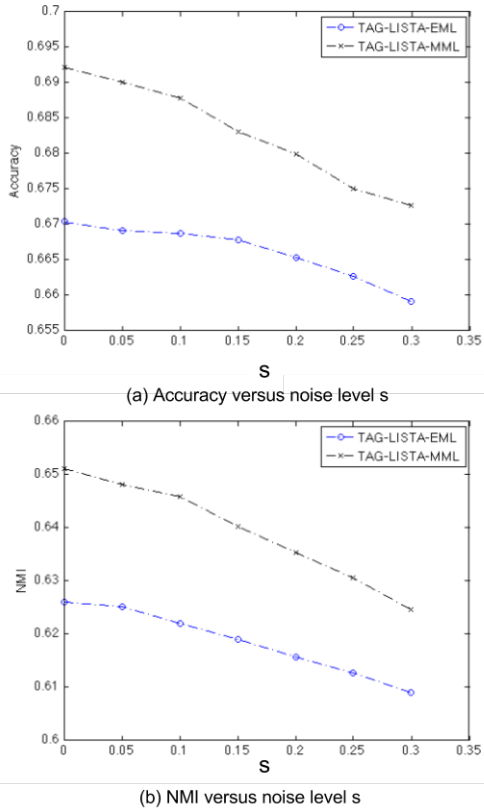


Figure 6: The clustering accuracy and NMI plots of TAGnet-EML/TAGnet-MML versus the noise level s , on MNIST.

The training of DTAGnet-EML/DTAGnet-MML follows the same above process except for considering extra back-propagated gradients from task $C_k(\mathbf{Z}_k, \omega_k)$ in Stage k ($k = 1, 2$). After then, we test each $C_k(\mathbf{Z}_k, \omega_k)$ separately on their targeted task. Since in DTAGnet, each auxiliary task is also jointly optimized with its input intermediate feature \mathbf{Z}_k , which differentiate our methodology substantially from [23], there is no surprise to see in Table 2 that each auxiliary task obtains much improved performances than [23]⁷. Most notably, the performances of the overall identity clustering task witness **a very impressive boost of around 7% in accuracy**. We also test DTAGnet-EML/DTAGnet-MML with only $C_1(\mathbf{Z}_1, \omega_1)$ or $C_2(\mathbf{Z}_2, \omega_2)$ kept. Experiments ver-

ify that by adding auxiliary tasks gradually, the overall task keeps being benefited. Those auxiliary tasks, when enforced together, can also reinforce each other mutually.

Table 2: Effects of incorporating auxiliary clustering tasks in DTAGnet-EML/DTAGnet-MML

Method	Stage I		Stage II		confusion	
	Task	Acc	Task	Acc	Task	Acc
DTAGnet-EML	/	/	/	/	Identity	0.2176
	Pose	0.5067	/	/	Identity	0.2303
	/	/	Expression	0.3676	Identity	0.2507
	Pose	0.5407	Expression	0.4027	Identity	0.2833
DTAGnet-MML	/	/	/	/	Identity	0.2347
	Pose	0.5251	/	/	Identity	0.2635
	/	/	Expression	0.3988	Identity	0.2858
	Pose	0.5538	Expression	0.4231	Identity	0.3021

Table 3: Effects of varying target cluster numbers of auxiliary tasks in DTAGnet-EML/DTAGnet-MML

Method	#clusters in Stage I	#clusters in Stage II	Overall Accuracy
DTAGnet-EML	4	4	0.2827
	8	8	0.2813
	12	12	0.2802
	20	20	0.2757
DTAGnet-MML	4	4	0.3030
	8	8	0.3006
	12	12	0.2927
	20	20	0.2805

One might be curious that, **which one matters more in the performance boost**: the deeply task-specific architecture that brings extra discriminative feature learning, or the proper design of auxiliary tasks that capture the intrinsic data structure characterized by attributes?

To answer this important question, we vary the target cluster number in either $C_1(\mathbf{Z}_1, \omega_1)$ or $C_2(\mathbf{Z}_2, \omega_2)$, and re-conduct the experiments. Table 3 reveals that more auxiliary tasks, even those without any straightforward task-specific interpretation (e.g., partitioning the Multi-PIE subset into 4, 8, 12 or 20 clusters hardly makes semantic sense), may still help gain better performances. It is comprehensible that they simply promote more discriminative feature learning in a low-to-high, coarse-to-fine scheme. In fact, it is a complementary observation to the conclusion found in classification [13]. On the other hand, at least in this specific case, while the target cluster numbers of auxiliary tasks get closer to the ground-truth (5 and 6 here), the models seem to achieve the best performances. We conjecture that when properly “matched”, every hidden representation in each layer is in fact most suited for clustering the attributes corresponding to the layer of interest. The whole model can be resembled to the problem of sharing low-level feature filters among several relevant high-level tasks in convolutional networks [8], but in a distinct context.

⁶In fact, although claimed to be applicable to multiple attributes, [23] only examined the first level features for pose clustering without considering expressions, since it relied on a warping technique to pre-process images, that gets rid of most expression variability.

⁷In [23] Table. 2, it reports that the best accuracy of pose clustering task falls around 28%, using the most suited layer features.

We hence conclude that, the deeply-supervised fashion shows to be helpful for the deep clustering models, even when there are no explicit attributes for constructing a practically meaningful hierarchical clustering problem. However, it is preferable to exploit those attributes when available, as they lead to not only superior performances but more clearly interpretable models. The learned intermediate features can be potentially utilized for multi-task learning [24].

6 Conclusion

In this paper, we present a deep learning-based clustering framework. Trained from end to end, it features a task-specific deep architecture inspired by the sparse coding domain expertise, which is then optimized under clustering-oriented losses. Such a well-designed architecture leads to more effective initialization and training, and significantly outperforms generic architectures of the same parameter complexity. The model could be further interpreted and enhanced, by introducing auxiliary clustering losses to the intermediate features. Extensive experiments verify the effectiveness and robustness of the proposed models.

References

- [1] M. Aharon, M. Elad, and A. Bruckstein. K-svd: An algorithm for designing overcomplete dictionaries for sparse representation. *Signal Processing, IEEE Transactions on*, 2006.
- [2] A. Beck and M. Teboulle. A fast iterative shrinkage-thresholding algorithm for linear inverse problems. *SIAM Journal on Imaging Sciences*, 2(1):183–202, 2009.
- [3] C. Biernacki, G. Celeux, and G. Govaert. Assessing a mixture model for clustering with the integrated completed likelihood. *Pattern Analysis and Machine Intelligence, IEEE Transactions on*, 22(7):719–725, 2000.
- [4] G. Chen. Deep learning with nonparametric clustering. *arXiv preprint arXiv:1501.03084*, 2015.
- [5] B. Cheng, J. Yang, S. Yan, Y. Fu, and T. S. Huang. Learning with l1 graph for image analysis. *Image Processing, IEEE Transactions on*, 19(4):858–866, 2010.
- [6] C. Cortes and V. Vapnik. Support-vector networks. *Machine Learning*, 20(3):273–297, 1995.
- [7] J. Donahue, Y. Jia, O. Vinyals, J. Hoffman, N. Zhang, E. Tzeng, and T. Darrell. Decaf: A deep convolutional activation feature for generic visual recognition. *arXiv preprint arXiv:1310.1531*, 2013.
- [8] X. Glorot, A. Bordes, and Y. Bengio. Domain adaptation for large-scale sentiment classification: A deep learning approach. In *International Conference on Machine Learning (ICML)*, pages 513–520, 2011.
- [9] K. Gregor and Y. LeCun. Learning fast approximations of sparse coding. In *International Conference on Machine Learning (ICML)*, pages 399–406, 2010.
- [10] R. Gross, I. Matthews, J. Cohn, T. Kanade, and S. Baker. Multi-pie. *Image and Vision Computing*, 28(5), 2010.
- [11] G. Hinton, S. Osindero, and Y.-W. Teh. A fast learning algorithm for deep belief nets. *Neural computation*, 2006.
- [12] A. Krizhevsky, I. Sutskever, and G. E. Hinton. Imagenet classification with deep convolutional neural networks. In *NIPS*, pages 1097–1105, 2012.
- [13] C.-Y. Lee, S. Xie, P. Gallagher, Z. Zhang, and Z. Tu. Deeply-supervised nets. *arXiv preprint arXiv:1409.5185*, 2014.
- [14] T. Li and C. Ding. The relationships among various nonnegative matrix factorization methods for clustering. In *ICDM*, pages 362–371. IEEE, 2006.
- [15] X. Li, K. Zhang, and T. Jiang. Minimum entropy clustering and applications to gene expression analysis. In *CSB*, pages 142–151. IEEE, 2004.
- [16] J. Mairal, F. Bach, and J. Ponce. Task-driven dictionary learning. *Pattern Analysis and Machine Intelligence, IEEE Transactions on*, 34(4):791–804, 2012.
- [17] A. Y. Ng, M. I. Jordan, Y. Weiss, et al. On spectral clustering: Analysis and an algorithm. *NIPS*, 2:849–856, 2002.
- [18] F. Nie, D. Xu, I. W. Tsang, and C. Zhang. Spectral embedded clustering. In *International Joint Conference on Artificial Intelligence (IJCAI)*, pages 1181–1186, 2009.
- [19] R. Pascanu, T. Mikolov, and Y. Bengio. On the difficulty of training recurrent neural networks. In *International Conference on Machine Learning (ICML)*, pages 1310–1318, 2013.
- [20] V. Roth and T. Lange. Feature selection in clustering problems. In *NIPS*, 2003.
- [21] I. Sutskever, J. Martens, G. Dahl, and G. Hinton. On the importance of initialization and momentum in deep learning. In *International Conference on Machine Learning (ICML)*, pages 1139–1147, 2013.
- [22] F. Tian, B. Gao, Q. Cui, E. Chen, and T.-Y. Liu. Learning deep representations for graph clustering. In *Twenty-Eighth AAAI Conference on Artificial Intelligence*, 2014.
- [23] G. Trigeorgis, K. Bousmalis, S. Zafeiriou, and B. Schuller. A deep semi-nmf model for learning hidden representations. In *International Conference on Machine Learning (ICML)*, pages 1692–1700, 2014.
- [24] Y. Wang, D. Wipf, Q. Ling, W. Chen, and I. Wassail. Multi-task learning for subspace segmentation. In *International Conference on Machine Learning (ICML)*, 2015.
- [25] Z. Wang, Y. Yang, S. Chang, J. Li, S. Fong, and T. S. Huang. A joint optimization framework of sparse coding and discriminative clustering. In *International Joint Conference on Artificial Intelligence (IJCAI)*, 2015.
- [26] J. Wright, A. Y. Yang, A. Ganesh, S. S. Sastry, and Y. Ma. Robust face recognition via sparse representation. *Pattern Analysis and Machine Intelligence, IEEE Transactions on*, 31(2):210–227, 2009.
- [27] L. Xu, J. Neufeld, B. Larson, and D. Schuurmans. Maximum margin clustering. In *NIPS*, pages 1537–1544, 2004.
- [28] Y. Yang, Z. Wang, J. Yang, J. Wang, S. Chang, and T. S. Huang. Data clustering by laplacian regularized l1-graph. In *Twenty-Eighth AAAI Conference on Artificial Intelligence*, 2014.
- [29] B. Zhao, F. Wang, and C. Zhang. Efficient maximum margin clustering via cutting plane algorithm. In *SIAM International Conference on Data Mining (SDM)*, pages 751–762, 2008.
- [30] M. Zheng, J. Bu, C. Chen, C. Wang, L. Zhang, G. Qiu, and D. Cai. Graph regularized sparse coding for image representation. *Image Processing, IEEE Transactions on*, 20(5):1327–1336, 2011.